The ISME Journal, 2024, **18(1)**, wrae093
https://doi.org/10.1093/ismejo/wrae093
Advance access publication: 31 May 2024
Brief Communication

Lytic and temperate phage naturally coexist in a dynamic population model

Ofer Kimchi[1], Yigal Meir[2,3], Ned S. Wingreen[1,4,*]

[1]Lewis-Sigler Institute for Integrative Genomics, Princeton University, Princeton, NJ 08544, USA
[2]Department of Physics, Ben-Gurion University, Be'er Sheva 84105, Israel
[3]Department of Physics, Princeton University, Princeton, NJ 08544, USA
[4]Department of Molecular Biology, Princeton University, Princeton, NJ 08544, USA

*Corresponding author: Ned S. Wingreen, Lewis-Sigler Institute for Integrative Genomics, Princeton University, Princeton, NJ 08544, USA.
Email: wingreen@princeton.edu

Abstract

When phage infect their bacterial hosts, they may either lyse the cell and generate a burst of new phage, or lysogenize the bacterium, incorporating the phage genome into it. Phage lysis/lysogeny strategies are assumed to be highly optimized, with the optimal tradeoff depending on environmental conditions. However, in nature, phage of radically different lysis/lysogeny strategies coexist in the same environment, preying on the same bacteria. How can phage preying on the same bacteria coexist if one is more optimal than the other? Here, we address this conundrum within a modeling framework, simulating the population dynamics of communities of phage and their lysogens. We find that coexistence between phage of different lysis/lysogeny strategies is a natural outcome of chaotic population dynamics that arise within sufficiently diverse communities, which ensure no phage is able to absolutely dominate its competitors. Our results further suggest a bet-hedging mechanism at the level of the phage pan-genome, wherein obligate lytic (virulent) strains typically outcompete temperate strains, but also more readily fluctuate to extinction within a local community.

Keywords: phage, lysogen, ecology, model, virulent, lytic, temperate, coexistence

Phage—viruses that infect bacteria—are subject to strong evolutionary pressures. One optimization axis is the lysis–lysogeny decision phage face when infecting a bacterium. Upon infection, phage can either lyse the bacterium, generating a burst of phage progeny, or lysogenize it, incorporating the phage genome into the bacterium. The resulting lysogen is generally immune to subsequent infection by the same class of phage [1, 2].

Obligate lytic phage, such as *Escherichia coli* phage T4, never lysogenize their bacterial hosts; temperate phage, such as the *E. coli* phages λ and P1 and the *Vibrio cholerae* phage CTXφ, can perform either lysis or lysogeny upon infection [3]. The optimal lysis/lysogeny tradeoff depends on environmental conditions [4, 5]: given abundant susceptible bacteria, phage do better by performing lysis; when these bacteria are scarce, phage are better off lysogenizing their hosts [6]. However, lytic and temperate phage that prey on the same bacteria coexist with one another [7, 8]. How can they coexist if one is more optimal than the other?

Explanations for the coexistence of competing species generally rely on the idea that different species have different ecological niches, e.g. in terms of resources or space [9, 10]. In contrast, here we show that naturally arising chaotic population dynamics are sufficient for the coexistence of obligate lytic and temperate phage. These dynamics arise only within sufficiently diverse communities and are absent when a single obligate lytic and temperate strain compete.

We consider N_c phage classes preying on a single bacterial species (Fig. 1). Lysogens are immune to reinfection by a phage of the same class. Each phage population density P_{cf} is indexed by its immunity class c and strain f, i.e. the fraction of its infections leading to lysogeny. Strains with $f = 0$ are obligate lytic and have no associated lysogens. The population densities of phage P_{cf} and their associated lysogens L_{cf} change according to (see Fig. 1 for parameter definitions and more detail):

$$\frac{dP_{cf}}{dt} = \underbrace{b\gamma L_{cf}}_{\text{Induction}} - \underbrace{\left(\delta + k\sum_{c'} L_{c'}\right) P_{cf}}_{\text{Phage death and adsorption}} + \underbrace{kb\,(1-f)\,P_{cf}\sum_{c'\neq c} L_{c'}}_{\text{Phage growth through lysis}}, \quad (1)$$

$$\frac{dL_{cf}}{dt} = \underbrace{\alpha L_{cf}}_{\text{Lysogen growth}} - \underbrace{\gamma L_{cf}}_{\text{Induction}} - \underbrace{kL_{cf}\sum_{c'\neq c}\sum_{f'}(1-f')\,P_{c'f'}}_{\text{Lysogen death due to lysis}},$$

where $L_c = \sum_f L_{cf}$. Equations (1) are a natural simplification of more comprehensive models which produce similar results; see Supplementary Sections S2 and S3, and Fig. S1. Although we focus on symmetric systems for simplicity and clarity, our results throughout are robust to heterogeneities in all parameters (Figs S3 and S12).

When a single obligate lytic strain and a single temperate strain compete, one or the other goes extinct depending on whether they are of the same or different classes (Fig. S2). However, when multiple temperate strains compete, we observe sustained chaotic dynamics (Figs 2a and S3a; Supplementary Section S4). These chaotic dynamics are robust to variations in parameter values and

Received: 4 March 2024. **Revised:** 14 May 2024. **Accepted:** 30 May 2024

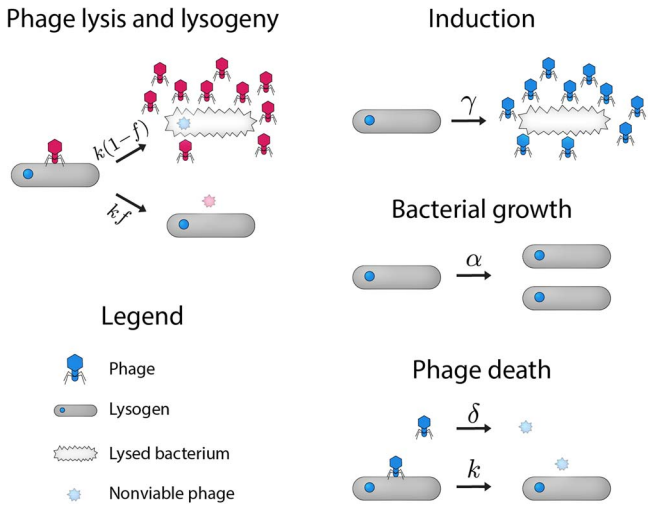

Figure 1. Model overview. A pictorial representation of the simplified model described by equations (1). Phage of different immunity classes are represented by different colors. Here, we disallow double lysogens and treat the population of sensitive (non-lysogenic) bacteria as negligible (see main text and Supplementary Section S2). Bacteria grow at a rate α, and are limited by phage predation rather than resource limitation. Phage populations grow through lysis. Phage infect bacteria at a rate k, leading to either lysis or lysogeny. Phage strains within a class are distinguished by their (fixed) fraction of infections that lead to lysogeny, denoted by f. If the phage performs lysis, it creates b new copies of the phage and kills the bacterium. Lysogens are immune to reinfection by a phage of the same class, and are spontaneously induced to undergo lysis at a rate γ. Phage die (or migrate away) at a rate δ, and phage that attempt to infect immune lysogens also die. Values for parameters are motivated by [11, 12] (see Supplementary Section S1).

parameter heterogeneity, with almost no simulations resulting in steady-state behavior (Figs S10, S11, S12). We hypothesized that these frequent large variations in populations (or "boom and bust" cycles) could lead to an opportunity for obligate lytic phage.

Obligate lytic strains are best able to capitalize on periods of phage population growth, outcompeting temperate strains of the same immunity class because they turn all bacterial hosts they infect into new phage (Fig. 2b; arrow). Indeed, when an obligate lytic strain was introduced into the simulations of Fig. 2a, it typically dominated over the temperate strain of the same class (Fig. 2b). At the same time, both strains persisted at high population densities, with little change in the behavior of phage of other immunity classes.

How do temperate phage persist if obligate lytic phage outcompete them during periods of phage expansion? We carried out simulations with three phage immunity classes, each with four strains (i.e. different values of f). We continued to see robust coexistence among all strains, and noticed a striking "bunching" effect when plotting the ratio of the temperate phage to their corresponding lysogen population densities (Fig. 2c). During periods of growth of a particular phage class, strains with smaller lysogeny fractions f typically outcompete those with larger f; however, P/L ratios were all nearly equal at the troughs (Fig. 2c). We traced this bunching effect to the induction of lysogens, which buffers temperate phage populations against periods of decline. To test this explanation quantitatively, we consider the behavior of an obligate lysogenic (or "dormant") phage with $f = 1$, whose dynamics are entirely determined by its respective lysogen. By setting $dP_{c1}/dt = 0$, we find a homeostatic population density for the phage, P^*_{c1}, which is approximately proportional to the strain's lysogen population density:

$$\frac{P^*_{c1}}{L_{c1}} = \frac{b\gamma}{k\,L_c + \delta}. \tag{2}$$

When the phage population density dips below P^*_{c1}, induction restores it back up, and when the phage population density rises above P^*_{c1}, phage death pushes it down. Equation (2) predicts the population densities of temperate phage at the troughs with reasonable accuracy (Fig. 2c); in fact, an even further simplified estimate of $b\gamma/\delta$ only overestimates the minimum population density ratios by a factor of ~2, compared to the overall variation in P/L of $\mathcal{O}\left(10^9\right)$ (We note that the simplified model of equations (1) retains a perfect memory of the initial ratios of lysogens of the same immunity class because dL_{cf}/dt is independent of f. This feature is incidental to the observed bunching effect; see Fig. S4.) The bunching effect, therefore, implies a population density "floor" for the temperate phage, protecting their populations during periods of decline.

In contrast, there is no population density floor for the obligate lytic phage, which have no corresponding lysogens, and therefore no induction buffering their populations (Fig. 2d). Therefore, although obligate lytic strains typically outcompete temperate strains, lytic strain population densities occasionally drop to very low levels. What then protects obligate lytic strains in nature from going extinct over long times?

In our model, the presence of more competitors leads to more stable behavior for all phage, raising the minima of obligate lytic strain populations. This effect arises because population minima are tied to the magnitude of fluctuations in the sum of the resources available to each phage; these fluctuations decrease as the number of distinct lysogenic species on which each phage can prey is increased (Figs 2e and S5). To explore this effect, we consider $N_c - 1$ classes each consisting of a single temperate strain, along with a single class with two strains (one obligate lytic and other temperate). Although the system dynamics are chaotic, the average population density $\langle P_{cf} \rangle$ of each phage with one strain in its immunity class agrees quantitatively with the steady-state fixed-point value (see Supplementary Section S5),

$$P^{ss}_{cf} = \frac{\alpha - \gamma}{k\ (N_c - 1)\,(1 - f)}, \tag{3}$$

i.e. the non-zero solution to $dP/dt = dL/dt = 0$ (Fig. 2f). The average of the obligate lytic phage population density is also reasonably well predicted by equation (3) with $f = 0$, despite the presence of a temperate strain of the same immunity class (Fig. 2f). The obligate lytic population density is on average orders of magnitude larger than that of the temperate phage in its immunity class, but only slightly smaller than the population densities of temperate phage of other immunity classes, as predicted by equation (3). Also as predicted by equation (3), as N_c is increased, the average population density of each strain decreases; however, the minimum population density of each strain *increases* and then plateaus with increasing N_c (Fig. 2f, inset). Thus, extinction becomes less likely in communities consisting of more phage immunity classes.

Our model makes several experimentally testable predictions. These can be tested with a community of several phage immunity classes, created following e.g. reference [2]. First, we predict chaotic population fluctuations when a sufficient number of phage of different immunity classes are placed within a chemostat with dilution rate slower than the phage-induced death rate of lysogens. Second, introducing an obligate lytic phage in the

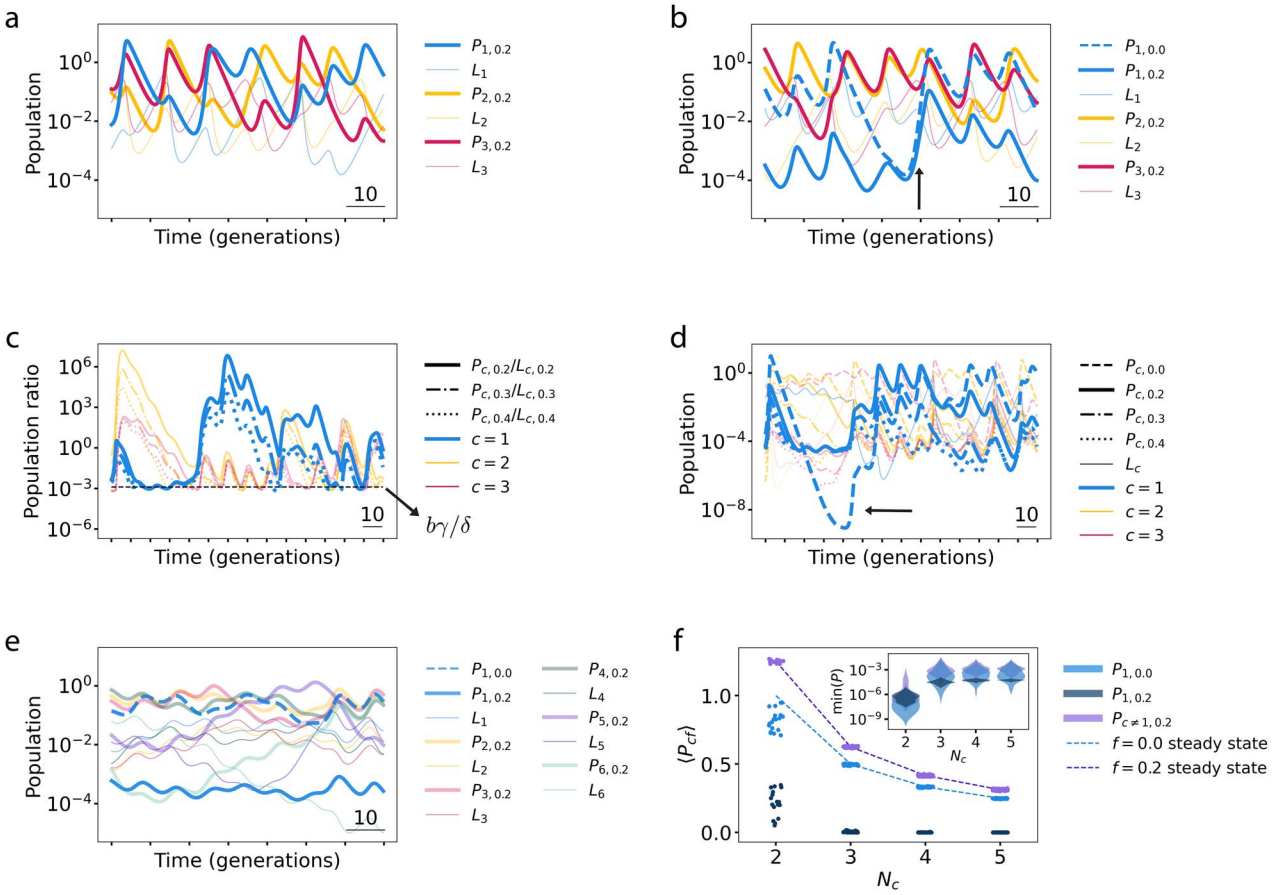

Figure 2. Population dynamics of coexisting obligate lytic and temperate phage. (**A**) Competition among multiple temperate phage classes ($N_c = 3$) leads to chaotic dynamics. (**B**) Chaos allows obligate lytic and temperate phage to coexist, with obligate lytic strains typically dominating over temperate strains of the same class. Arrow points to a growth period of phage of immunity class 1 (blue). (**C**) Simulation of $N_c = 3$ phage immunity classes each with one obligate lytic strain and three temperate strains; all strains coexist together. Here, temperate phage population densities are plotted normalized by their respective lysogen population density. In periods of growth of a particular phage immunity class, the more lytic strains dominate, but phage-to-lysogen population density ratios "bunch" together at troughs, with a population density floor predicted by equation (2) (black dashed line). (**D**) Plot of population densities (rather than population density ratios) of simulation shown in (**C**). In order to compare the temperate phage population density floor with a population dip of an obligate lytic phage which lacks such a floor (arrow), lysogens of different strains of the same class were initialized with equal population densities (and remain equal indefinitely; see Fig. S4). (**E**) Increasing the number of phage classes (here to $N_c = 6$) generally leads to smaller population density variation. (**F**) Summary statistics across 50 simulations, each for 2000 generations. Each simulation competes $N_c - 1$ immunity classes, each consisting of a single temperate strain (purple), along with a single class with two strains: One obligate lytic (light blue), one temperate (dark blue). The steady-state fixed-point solutions for the phage population densities (equation (3); dashed curves) agree well with the average of the chaotic trajectories. Average phage population densities decrease with N_c (main figure, scatter plot) whereas minimum population densities increase with N_c (inset, violin plot). Simulations for $N_c = 2$ in which the obligate lytic phage fluctuated to extinction were excluded.

same immunity class as one of the temperate phages will lead to a substantial (albeit finite) decrease of the latter's population, with little effect on the behavior of the phage in other immunity classes. Third, obligate lytic phage will reach lower population minima than temperate phage. Finally, we predict that whereas the average phage populations will decrease with increased number of immunity classes N_c, the minimum phage populations taken over a long enough window will actually increase with N_c.

To address the robustness of these predictions to our simplifying approximations, we construct extensions of our model to more realistic systems including sensitive bacteria and double lysogens (Figs S6 and S7), heterogeneous lysogeny probabilities (Fig. S3b-c), obligate lytic phage with no temperate strain of the same immunity class (Fig. S3d), and a finite lysis time and coinfection-induced lysogeny [13, 14] (Fig. S8), all of which yield the same qualitative behavior. Finally, although we have focused on ecological dynamics in the absence of mutations, we expect our results to hold in laboratory experiments. Whereas bacterial populations can in some cases rapidly develop phage-resistant mutations, these are typically followed by compensatory mutations in the phage [15, 16]. Furthermore, resistance mutations typically carry a cost to bacteria such that they do not always arise in natural populations containing multiple phage strains [17]. In particular, the presence of other competing bacteria could thus restrict the survival of bacteria with costly phage-resistance mutations. Similarly, although phage can over time evolve to infect new hosts, we expect these evolutionary dynamics to be much slower than the ecological dynamics considered here [18]. Nevertheless, further studies modeling simultaneous time-dependent ecological dynamics and evolution may fruitfully reveal interactions between these dynamics.

Contrary to prior work finding, optimal phage strategies survive as sub-optimal strategies go extinct [11, 19], our results suggest coexistence of different strategies may be commonplace. With a single obligate lytic phage strain and a single temperate phage strain of different immunity classes (i.e. a model akin to that

considered in Fig. S2, bottom row), prior work showed static steady-state coexistence is possible for certain parameter combinations, such as when the obligate lytic phage burst size and infection rate are smaller than those of the temperate phage [20]; steady-state coexistence was also seen for phage of the same immunity class [21]. Our work expands beyond these scenarios, finding for multiple classes a qualitatively different form of coexistence mediated by chaos. Although in principle, a steady-state fixed point can be found as a solution to equation (1) (see equation (3)), its basin of attraction is so small that we predict any real instantiation of such a system will undergo robust chaotic dynamics (see also Supplementary Section S4 and Figs S10 and S11). Species coexistence mediated by chaotic population dynamics has been studied theoretically in other contexts including generalized Lotka-Volterra models and has been shown to arise from heterogeneities of large systems [10, 22, 23]; here, chaos arises naturally from the interactions of phage with their lysogens and is robust to varying degrees of parameter heterogeneity, including a lack thereof (Fig. S12).

Our results suggest a natural bet-hedging mechanism for phage on the pan-genome level. When susceptible bacteria are plentiful, obligate lytic strains thrive, while their temperate cousins of the same immunity class persist at lower populations. When conditions worsen, however, temperate strains can outcompete obligate lytic strains. Thus, obligate lytic strains, typically dominant, would be first to go extinct. Here, the bet-hedging is not a product of the behavior of individual organisms, but rather a feature of competing strains within a larger, genetically related, population.

Acknowledgements

We thank Jonathan Levine for useful discussions.

Author contributions

All the authors designed research, analyzed data, and wrote the article. O.K. wrote Python code.

Supplementary material

Supplementary material is available at *The ISME Journal* online.

Conflict of interest

The authors declare no competing interests.

Funding

This work was supported in part by grant number DAF2024-342781 from the Chan Zuckerberg Initiative DAF, an advised fund of Silicon Valley Community Foundation (N.S.W.), by the National Science Foundation through the Center for the Physics of Biological Function (PHY-1734030), and by the Peter B. Lewis '55 Lewis-Sigler Institute/Genomics Fund through the Lewis-Sigler Institute for Integrative Genomics at Princeton University (O.K.). This work was performed in part at Aspen Center for Physics, which is supported by National Science Foundation grant PHY-1607611.

Code availability

All code used to generate the results and figures in this study can be found at https://github.com/ofer-kimchi/lytic-temperate-coexistence.

Data availability

Data sharing not applicable to this article as no datasets were generated or analysed during the current study.

References

1. Boyd JSK. Immunity of lysogenic bacteria. *Nature* 1956;**178**:141. https://doi.org/10.1038/178141a0
2. Bondy-Denomy J, Qian J, Westra ER *et al.* Prophages mediate defense against phage infection through diverse mechanisms. *ISME J* 2016;**10**:2854–66. https://doi.org/10.1038/ismej.2016.79
3. Hobbs Z, Abedon ST. Diversity of phage infection types and associated terminology: the problem with 'lytic or lysogenic'. *FEMS Microbiol Lett* 2016;**363**:fnw047. https://doi.org/10.1093/femsle/fnw047
4. Maslov S, Sneppen K. Well-temperate phage: optimal bet-hedging against local environmental collapses. *Sci Rep* 2015;**5**:10523. https://doi.org/10.1038/srep10523
5. Howard-Varona C, Hargreaves KR, Abedon ST *et al.* Lysogeny in nature: mechanisms, impact and ecology of temperate phages. *ISME J* 2017;**11**:1511–20. https://doi.org/10.1038/ismej.2017.16
6. Wahl LM, Betti MI, Dick DW *et al.* Evolutionary stability of the lysis-lysogeny decision: Why be virulent? *Evolution* 2019;**73**:92–8. https://doi.org/10.1111/evo.13648
7. Breitbart M, Rohwer F. Here a virus, there a virus, everywhere the same virus? *Trends Microbiol* 2005;**13**:278–84. https://doi.org/10.1016/j.tim.2005.04.003
8. Pinto Y, Chakraborty M, Jain N *et al.* Phage-inclusive profiling of human gut microbiomes with Phanta. *Nat Biotechnol* 2024;**42**:651–62. https://doi.org/10.1038/s41587-023-01799-4
9. Haerter JO, Mitarai N, Sneppen K. Phage and bacteria support mutual diversity in a narrowing staircase of coexistence. *ISME J* 2014;**8**:2317–26. https://doi.org/10.1038/ismej.2014.80
10. Pearce MT, Agarwala A, Fisher DS. Stabilization of extensive fine-scale diversity by ecologically driven spatiotemporal chaos. *Proc Natl Acad Sci USA* 2020;**117**:14572–83. https://doi.org/10.1073/pnas.1915313117
11. Cortes MG, Krog J, Balázsi G. Optimality of the spontaneous prophage induction rate. *J Theor Biol* 2019;**483**:110005. https://doi.org/10.1016/j.jtbi.2019.110005
12. Wang IN. Lysis timing and bacteriophage fitness. *Genetics* 2006;**172**:17–26. https://doi.org/10.1534/genetics.105.045922
13. Yao T, Coleman S, Phuc TV *et al.* Bacteriophage self- counting in the presence of viral replication. *Proc Natl Acad Sci USA* 2021;**118**:e2104163118. https://doi.org/10.1073/pnas.2104163118
14. Stough JMA, Tang X, Krausfeldt LE *et al.* Molecular prediction of lytic vs lysogenic states for microcystis phage: Metatranscriptomic evidence of lysogeny during large bloom events. *PLoS One* 2017;**12**:e0184146. https://doi.org/10.1371/journal.pone.0184146
15. Borin JM, Lee JJ, Lucia-Sanz A *et al.* Rapid bacteria-phage coevolution drives the emergence of multiscale networks. *Science* 2023;**382**:674–8. https://doi.org/10.1126/science.adi5536
16. Tamar ES, Kishony R. Multistep diversification in spatiotemporal bacterial-phage coevolution. *Nat Commun* 2022;**13**:7971. https://doi.org/10.1038/s41467-022-35351-w
17. Oechslin F. Resistance development to bacteriophages occurring during bacteriophage therapy. *Viruses* 2018;**10**:351. https://doi.org/10.3390/v10070351
18. Guyader S, Burch CL. Optimal foraging predicts the ecology but not the evolution of host specialization in bacteriophages.

PLoS One 2008;**3**:e1946. https://doi.org/10.1371/journal.pone.0001946

19. Cheong KH, Wen T, Benler S *et al.* Alternating lysis and lysogeny is a winning strategy in bacteriophages due to Parrondo's paradox. *Proc Natl Acad Sci USA* **119**:2022. https://doi.org/10.1073/pnas.2115145119
20. Stewart FM, Levin BR. The population biology of bacterial viruses: Why be temperate. *Theor Popul Biol* 1984;**26**:93–117. https://doi.org/10.1016/0040-5809(84)90026-1
21. Li G, Cortez MH, Dushoff J *et al.* When to be temperate: on the fitness benefits of lysis vs. *lysogeny Virus Evolution* 2020;**6**:veaa042. https://doi.org/10.1093/ve/veaa042.
22. Huisman J, Weissing FJ. Biodiversity of plankton by species oscilations and chaos. *Nature* 1999;**402**:407–10. https://doi.org/10.1038/46540
23. de Pirey TA, Bunin G. Many-species ecological fluctuations as a jump process from the brink of extinction. *Physical Review X* 2024;**14**:11037. https://doi.org/10.1103/PhysRevX.14.011037

Supplementary Information

Supplemental figures

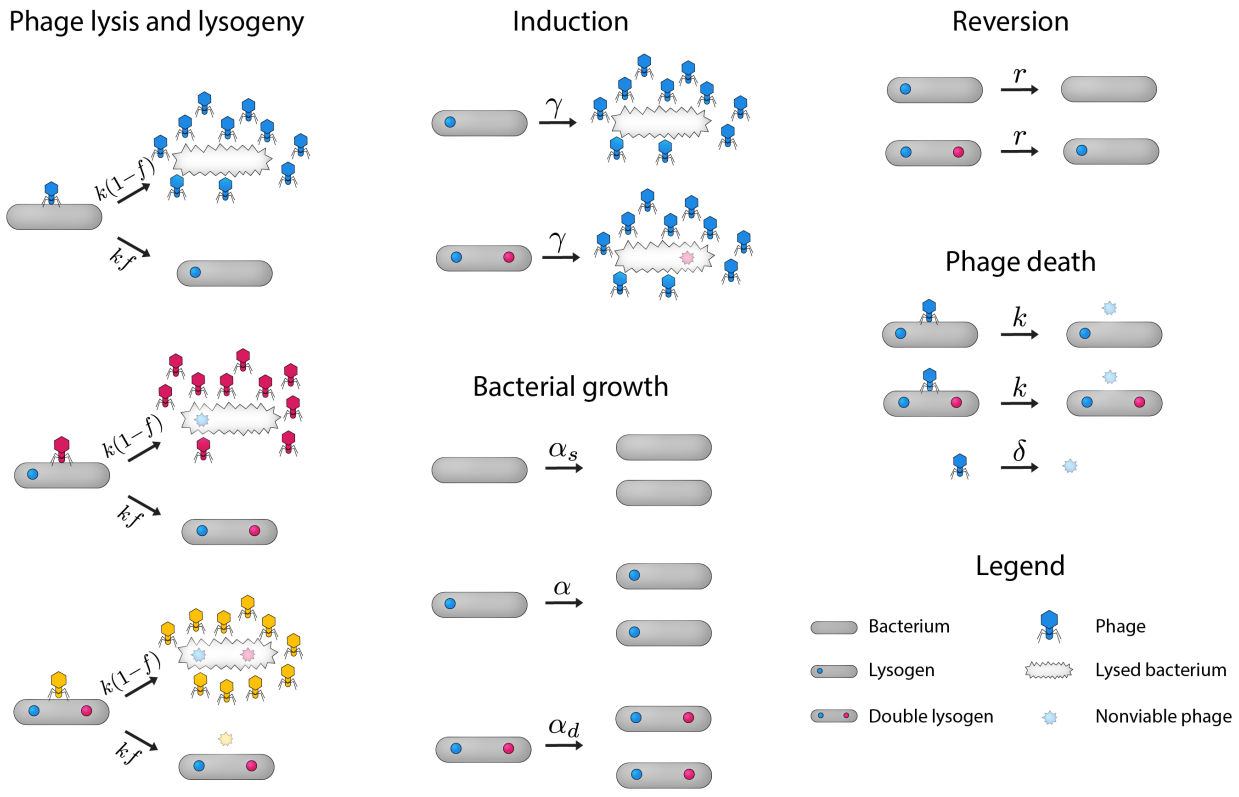

Figure S1: **Comprehensive model overview.** A pictoral representation of the full model described by equations (S3). Phage of different immunity classes are represented by different colors.

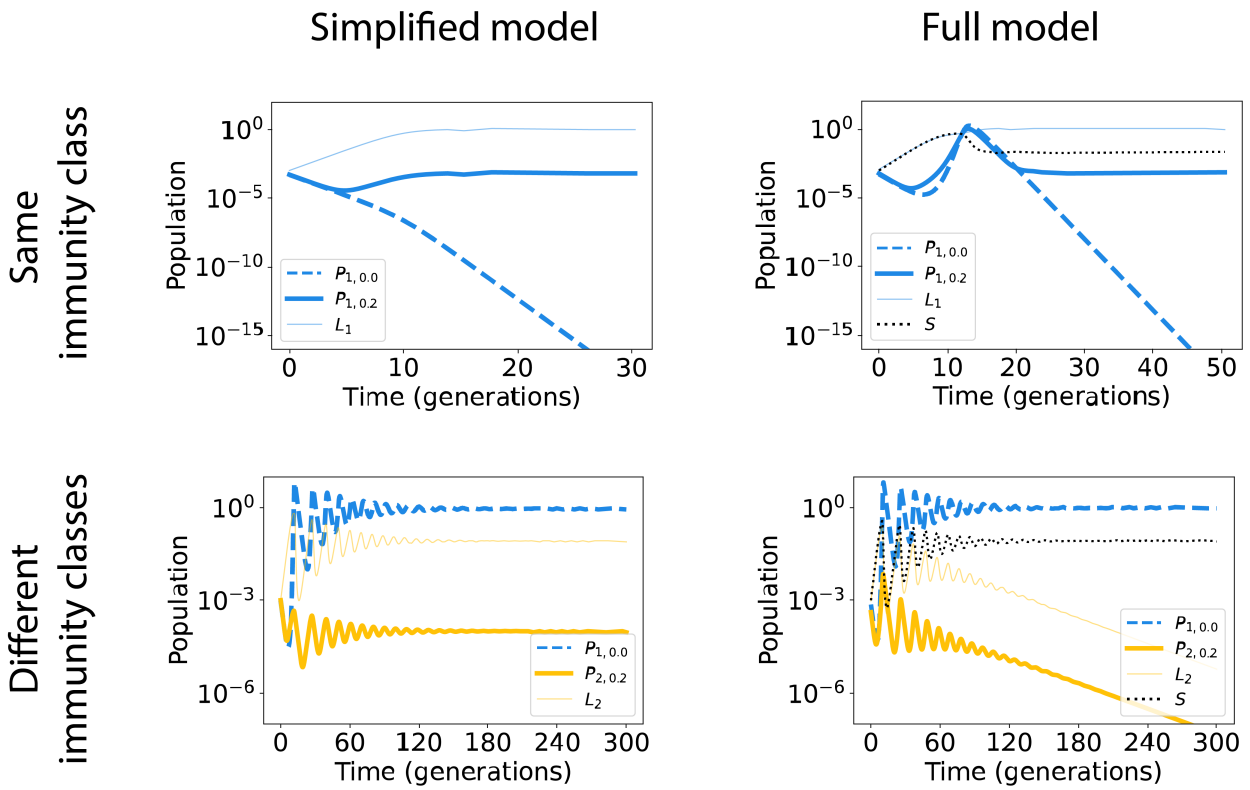

Figure S2: **Competition between a single obligate lytic strain and a single temperate strain.** We show the results of competition between a single obligate lytic strain and a single temperate strain of either the same (top row) or different (bottom row) immunity classes. Both the simplified (left column; equations (1)) and more comprehensive (i.e. including sensitive bacteria; Eqs. (S3) and (S4); right column) models show that when the two strains are of the same immunity class, the obligate lytic strain goes extinct, while the temperate strain survives. When the two strains are of different immunity classes, the obligate lytic phage dominates over the temperate phage as the temperate-phage lysogens are not immune to the lytic phage. In the comprehensive model, the sensitive strain outcompetes the lysogens as the former has a slightly higher growth rate, leading the temperate strain in that model to go extinct; in the simplified model, lysogens survive and so the temperate strain persists as a result of induction. In equations (S3) and (S4) for the full model, the carrying capacity of bacteria was set to $K = 1$.

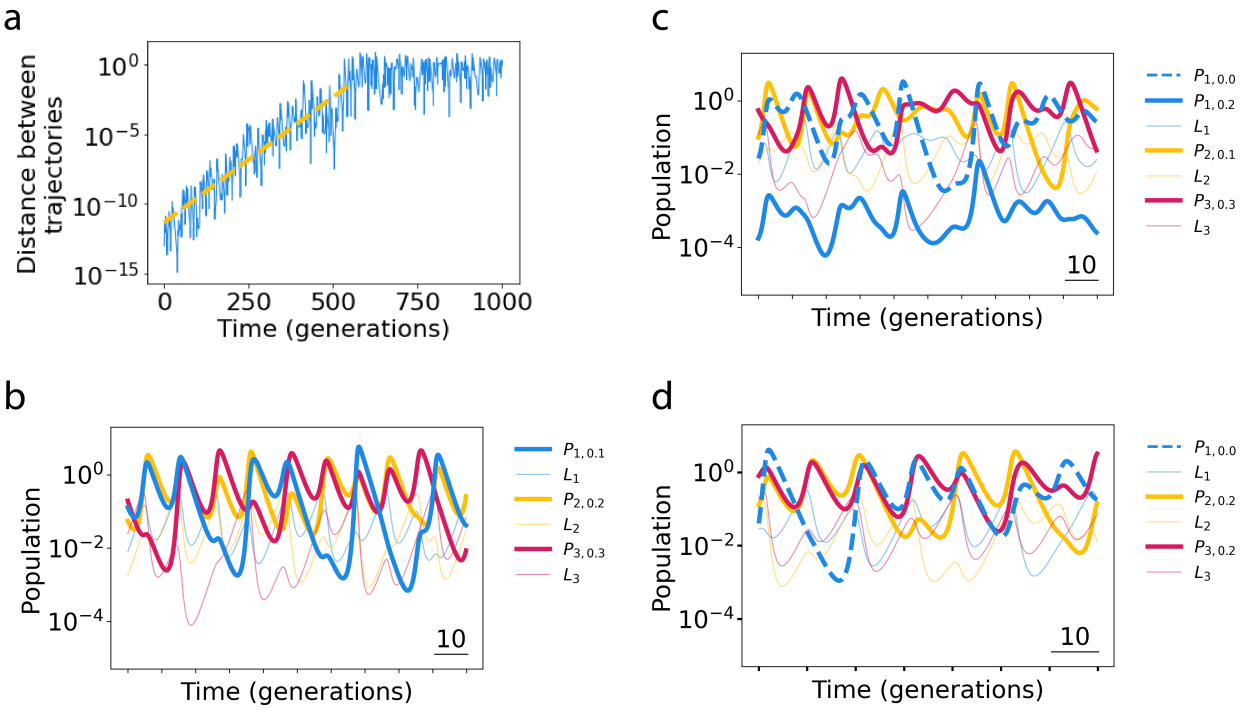

Figure S3: **Trajectories display robust chaotic dynamics. a,** Three temperate phage of different immunity classes were simulated. Then, a second simulation with nearly identical initial conditions was run (initial phage population densities were set to be 10^{-13} larger). We plot in blue the distance between the two trajectories of the first immunity class, $\sqrt{(P_{1,0.2} - P'_{1,0.2})^2}$. The initial portion of the plot is fit to an exponential, with Lyapunov exponent 6×10^{-2} (yellow dashed line). That nearby trajectories diverge exponentially is a hallmark of chaotic dynamics. **b, c,** Chaotic dynamics persist with heterogeneous lysogeny fractions f, with little qualitative difference from the case of homogeneous f (Fig. 2a-b). **d,** Chaotic dynamics are qualitatively unchanged if the obligate lytic strain is not paired with a temperate strain of the same immunity class. Here, bacteria labeled L_1 are non-lysogenic (with induction rate $\gamma = 0$) but are immune to infection by phage $P_{1,0}$.

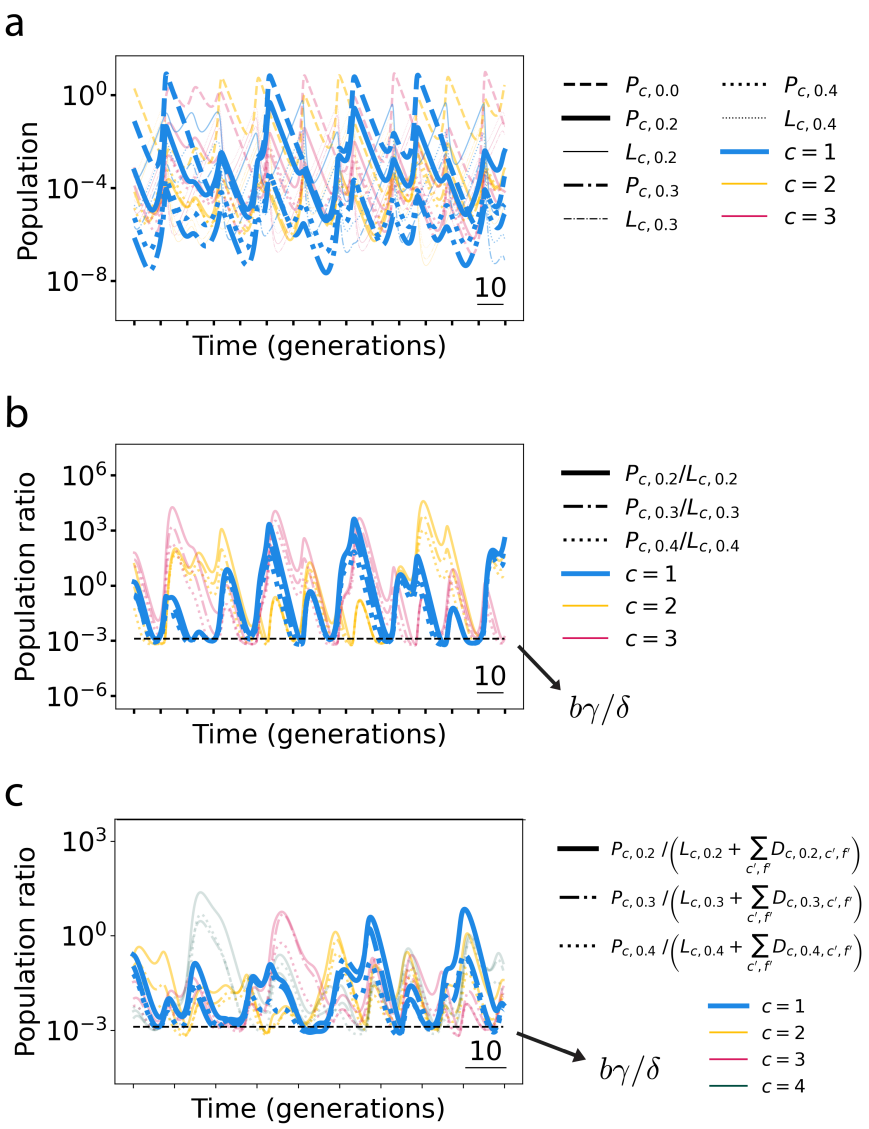

Figure S4: **Bunching effect with heterogeneous initial lysogen population densities. a,** Simulations performed as in Fig. 2c-d, i.e. with $N_c = 3$ phage immunity classes each with one obligate lytic strain and three temperate strains, but with one difference: here, initial lysogen population densities were chosen randomly over a range of ~ 2 orders of magnitude. Since in the simplified model, equations (1), $dL_{c,f}/dt$ is independent of f, the lysogens of different strains of the same immunity class vary in lockstep together, and the system retains a perfect memory of their initial population density ratios. **b,** The bunching effect at phage population troughs is independent of this memory, and the ratio of the population density of each phage to the population density of its respective lysogen is qualitatively unchanged compared to Fig. 2c. **c,** The full model (equations (S3)), which lacks this memory, displays the same bunching effect; furthermore, the population density floor is quantitatively unchanged from the simplified model, and is determined by the total population density of each phage strain's respective lysogens, including both single and double lysogens.

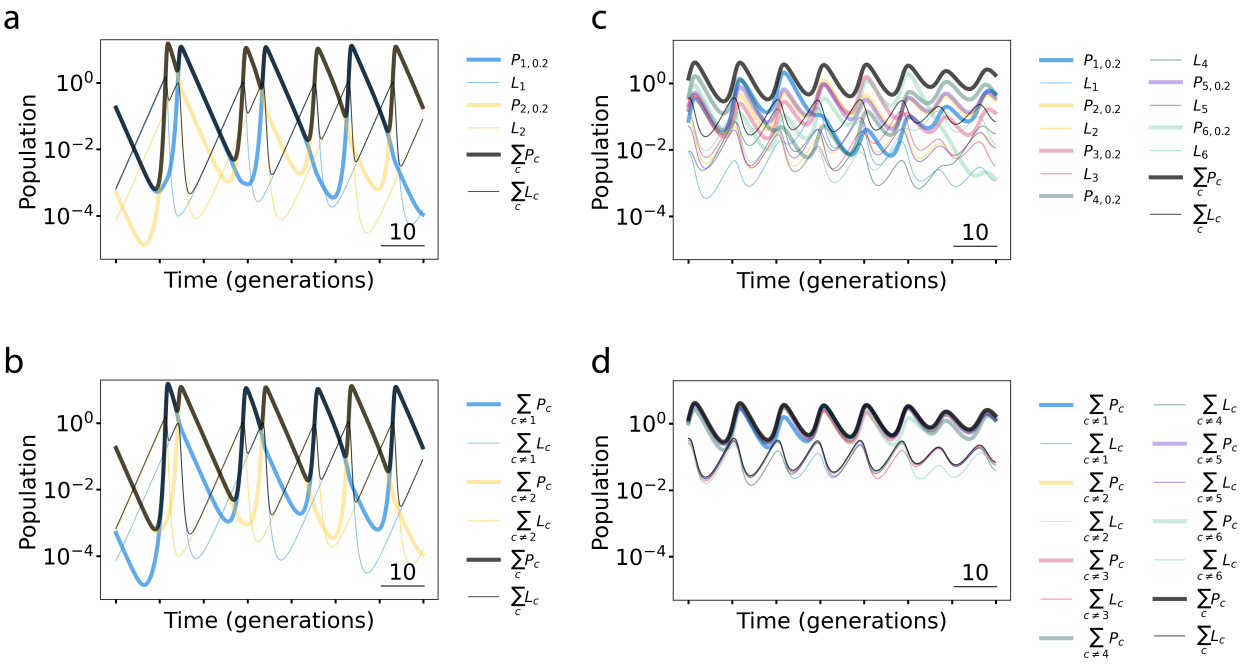

Figure S5: **Fluctuations decrease with more competing phage strains. a,c,** Representative simulations with two (panel a) or six (panel c) phage immunity classes showing fluctuations in both individual (colors) and overall (black) population densities. **b,d,** The same simulations as in panels a and c but with the summed population densities of all immunity classes but one visualized as distinct colors, demonstrating a decrease in variability with six immunity classes (panel d) compared to two (panel b).

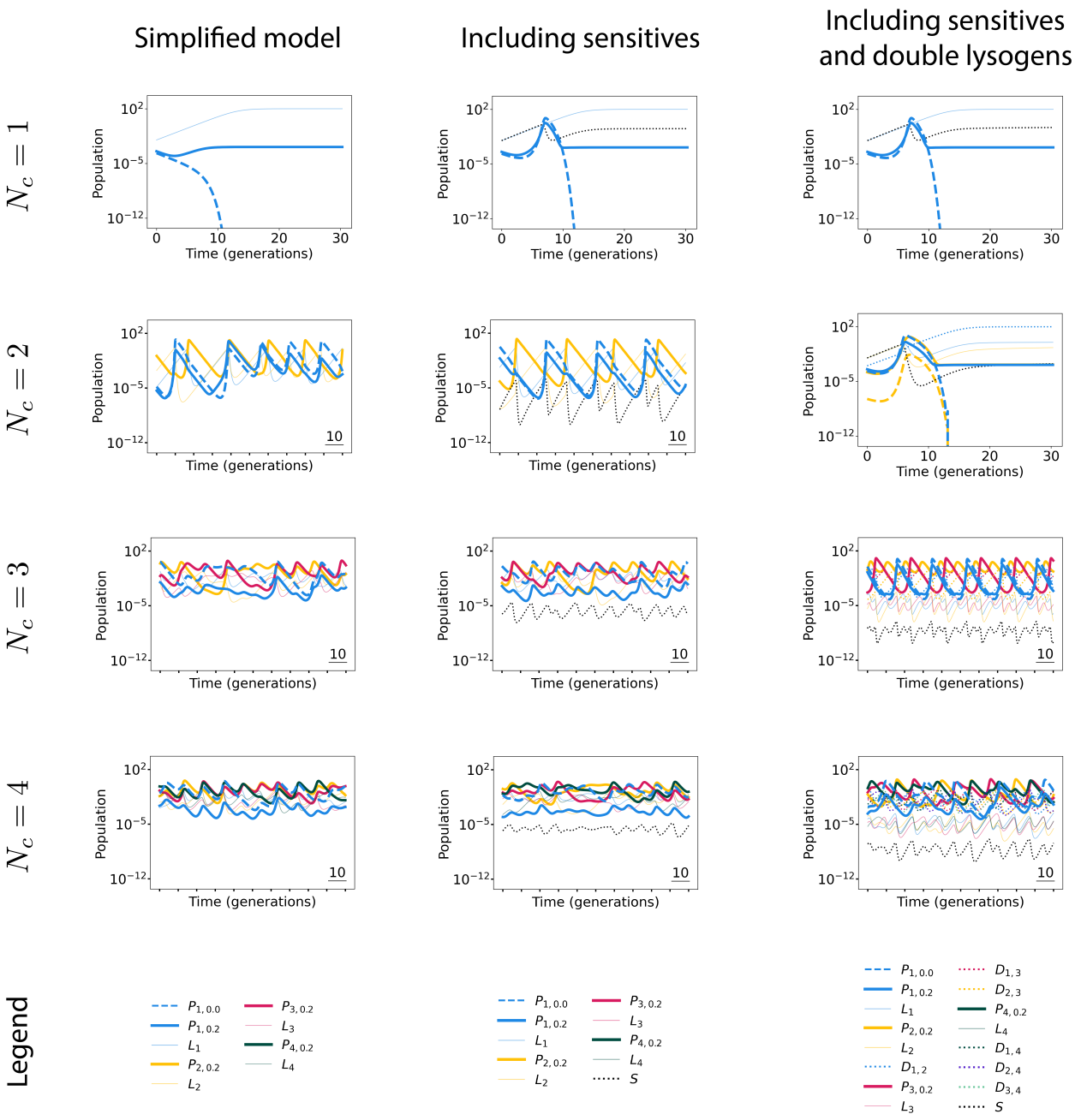

Figure S6: **Comparison of models with different degrees of simplification.** Simulation results are shown for the simplified model (equations (1), left column), the model including sensitive (i.e. non-lysogenic) bacteria (equations (S4), middle column), and the full model including both sensitive bacteria and double lysogens (equations (S3), right column). Each simulation has N_c competing phage immunity classes. One immunity class has both an obligate lytic strain and a temperate strain, while the other $N_c - 1$ immunity classes have a single temperate strain. Carrying capacity of bacteria, K, was set to 100 in the middle and right columns.

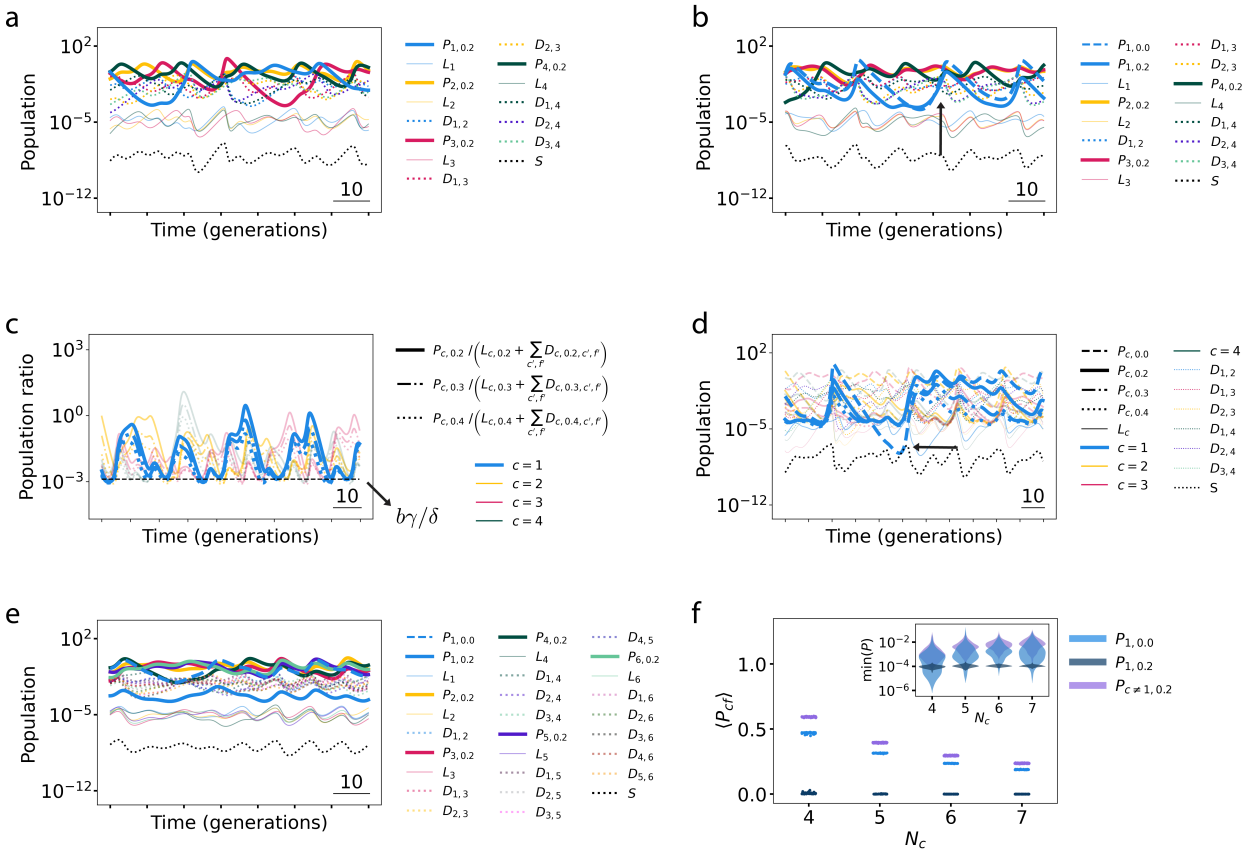

Figure S7: **Recapitulation of Fig. 2 using a more comprehensive model.** All panels as in Fig. 2, using equations (S3) in place of equations (1). $N_c = 2, 3$ are not included in panel f as they lead to oscillatory solutions.

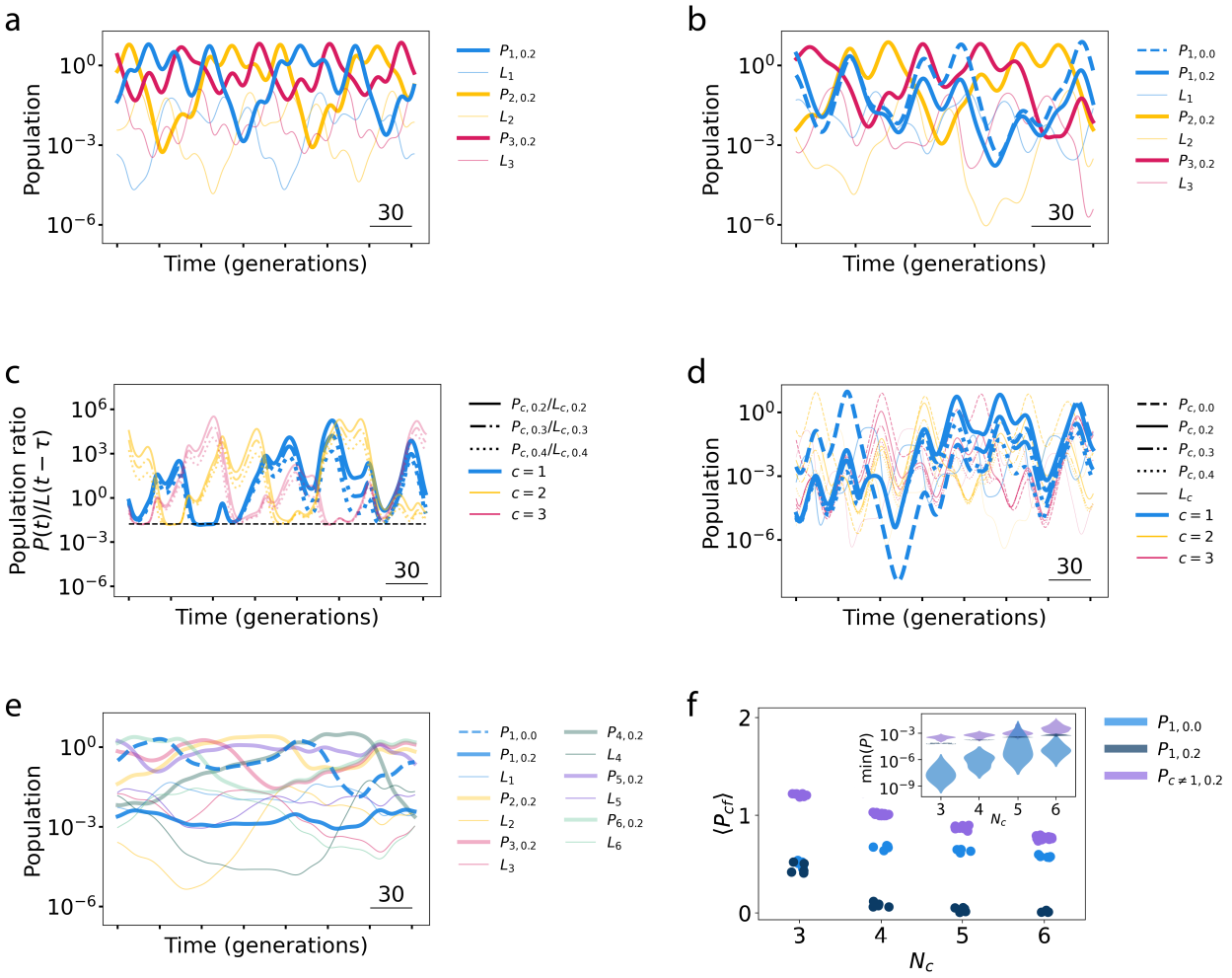

Figure S8: **Recapitulation of Fig. 2 incorporating a finite lysis time.** All panels as in Fig. 2, using equations (S5) in place of equations (1). $K = 0.2$ and $k = 1/N_c$ throughout; see Section S3. In panel c, phage population densities at time t are compared to lysogens at time $t - \tau$ where $\tau \approx 2.5$ generations is the time delay between phage infection and lytic burst; see Fig. S14 for ratio of $P(t)/L(t)$. $N_c = 2$ is not included in panel f as it leads to quasi-oscillatory solutions. Panel f shows summary statistics across 5 simulations, simulated for 5×10^3 generations each.

S1 Parameters

The values for the parameters used in the model are motivated by Cortes *et al.* (2019) [1]. Parameters setting the units for time and population density are the lysogen growth rate α and the infection rate constant k, which are both set to unity. The induction rate is small compared to the lysogen growth rate: $\gamma = 10^{-4}\alpha$. With this value of γ, induction of one lysogenic offspring will occur roughly 12 generations after lysogeny.

Our parameter choices differ from those of Cortes *et al.* in three main ways. First, while we consider finite nutrient conditions (and thus finite bacterial carrying capacities) in Section S2, we simplify the model in the main text to assume bacterial populations are exclusively limited by phage predation. Second, we assume a higher phage degradation rate than Cortes *et al.* by setting $\delta = \alpha$, accounting for both phage degradation and migration out of the local environment.

The third way our parameter choices differ from those of Cortes *et al.* regards the lysis time. Once a phage decides to undergo lysis, it creates many new phage virions. This process takes a significant amount of time, of the same order as a typical bacterial generation time. For example, phage λ has a period of ~ 50 minutes between infection and lysis of its *E. coli* host, roughly 2.5 times as long as the doubling time of *E. coli* in the same experiment (20 minutes) [2]. Below, we describe how a model with zero delay and a small burst size leads to the same overall phage growth rate as a model with a finite delay and larger burst size.

To model a finite lysis time explicitly, we could in principle modify equation (1) into a delay differential equation with a delay time τ:

$$\frac{dP_{c0}(t)}{dt} = k(b_\tau - 1)P_{c0}(t-\tau)\sum_{c'\neq c} L_{c'}(t-\tau) - \delta P_{c0}(t), \tag{S1}$$

where for simplicity, we have considered the obligate lytic phage ($f = 0$), and assumed it is the only strain in immunity class c. We have denoted the burst size in this model by b_τ to distinguish it from the burst size in the model with $\tau = 0$. Also for simplicity, we approximate the total lysogen population density susceptible to our strain of interest by a constant, L. We then have:

$$\frac{dP_{c0}(t)}{dt} = k(b_\tau - 1)LP_{c0}(t-\tau) - \delta P_{c0}(t). \tag{S2}$$

The solution to this equation approaches an exponential for large t. Keeping all other parameters equal (here we use $L = 0.2$), we find that the solution for finite τ is well-approximated by a model with $\tau = 0$ and a smaller burst size $b \equiv b_0$. The dependence of b on the time-delayed burst size b_τ and the length of the delay τ is shown in Fig. S9a. For realistic parameters, $\tau = 51$ min and $b_\tau = 170$ [2], we obtain an equivalent model with $\tau = 0$ and burst size $b = 13$ (rounded up from a best-fit value of 12.5). This simplified model with $\tau = 0$ gives a very good approximation to the results with a finite value of τ and a larger burst size, as shown in Fig. S9b. For the results of a model with finite lysis time and a corresponding large burst size, see Section S3.

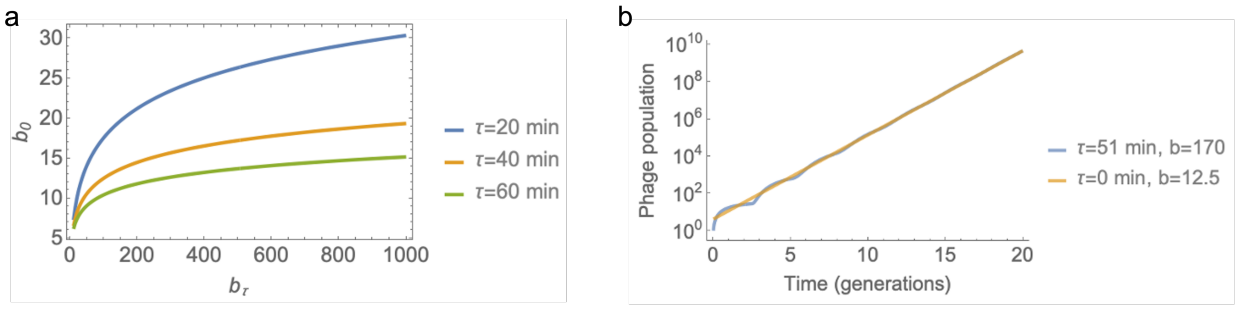

Figure S9: **A model with zero lysis time and a small burst size quantitatively approximates one with a finite lysis time and a larger burst size. a,** As a function of the true burst size b_τ for a given lysis time τ, the best-fit burst size for a model with zero lysis time, b_0, is shown. **b,** The solution to the delay-differential equation with $\tau = 51$ min and $b_\tau = 170$ is plotted alongsize the solution with $\tau = 0$ and $b_0 = 12.5$.

Parameter	Symbol	Default value	Unnormalized units
Infectivity	k	1	$(tc)^{-1}$
Lysogen growth rate	α	1	t^{-1}
Phage death rate	δ	1	t^{-1}
Induction rate	γ	10^{-4}	t^{-1}
Lysogeny fraction	f	0.2	None
Burst size	b	13	None

Table S1: **Parameters and their values (unless specified otherwise).** α and k set the units of time and population density; by setting these to unity, parameters are kept unitless. In the absence of such normalization, units would be given by the third column, where t represents units of time, and c units of concentration.

The full set of parameters used in our study is given in Table S1. In order to explore the robustness of our results to changes in these parameters, we performed one-dimensional parameter sweeps, exploring how coexistence and population density sizes changed in response to parameter variation. We used the $N_c = 6$ system, and kept all parameters but one as described in Table S1. One by one, we varied the following parameters: the lysogeny fraction f of all temperate phage; the lysogeny fraction f of temperate phage sharing an immunity class with an obligate lytic strain; the infectivity k, the induction rate γ, the burst size b, and the phage death rate δ. The results are shown in Fig. S10 and demonstrate robustness to parameter changes.

We additionally explored how the nature of coexistence – steady-state, oscillatory, or chaotic – changed as a result of parameter changes (Fig. S10a). We found robustness of the chaotic behavior observed to parameter changes, with the apparent exception of δ: varying δ by an order of magnitude in either direction yields oscillatory results for simulations lasting $> 10^4$ generations. To explore this behavior further, we measured the effect of more incremental changes in δ within this two-order-of-magnitude range, as well as the effect of changing the simulation time; results are shown in Fig. S11. For each δ and for a given simulation time of T generations, we examined the results in a window of $\min\{T, 420\}$ generations for evidence of oscillatory behavior, for 9 different initial conditions. Panels b-c of Fig. S11 show example chaotic trajectories for values of δ varying by nearly two orders of magnitude.

Initial conditions were chosen to be close to the predicted steady-state value while allowing for reasonable variation, as follows: Given the analytically predicted fixed point $(P^\star, L^\star)$ in the absence of obligate lytic phage, the initial conditions were given by multiplying $(3P^\star, L^\star)$ by a uniformly chosen random number between 0 and 1, and further multiplying P by a logarithmically chosen random number between 10^{-1} and 10^1. The 9 initial conditions used were kept consistent throughout Fig. S11. This procedure was used to generate initial conditions throughout the manuscript.

Finally, we explored how heterogeneity in the parameters can affect coexistence. Using the same $N_c = 6$ system, we varied the parameters b, k, f, and γ randomly – and independently for each phage/lysogen pair – from the general values in Table S1. We tested 10 random parameter sets at each one of 11 chosen fractional spreads ranging from 1% variation to 50%. For a given fractional spread σ, parameter values were chosen uniformly from within the range $1 \pm \sigma$ times their default value. Our results, shown in Fig. S12, show robust coexistence in these heterogeneous parameter systems. With 10% parameter variation, 9/10 simulations showed coexistence of all strains after $\sim$14,000 generations. Even with 50% parameter variation, an average of 4 phage strains continue to coexist after $\sim$14,000 generations.

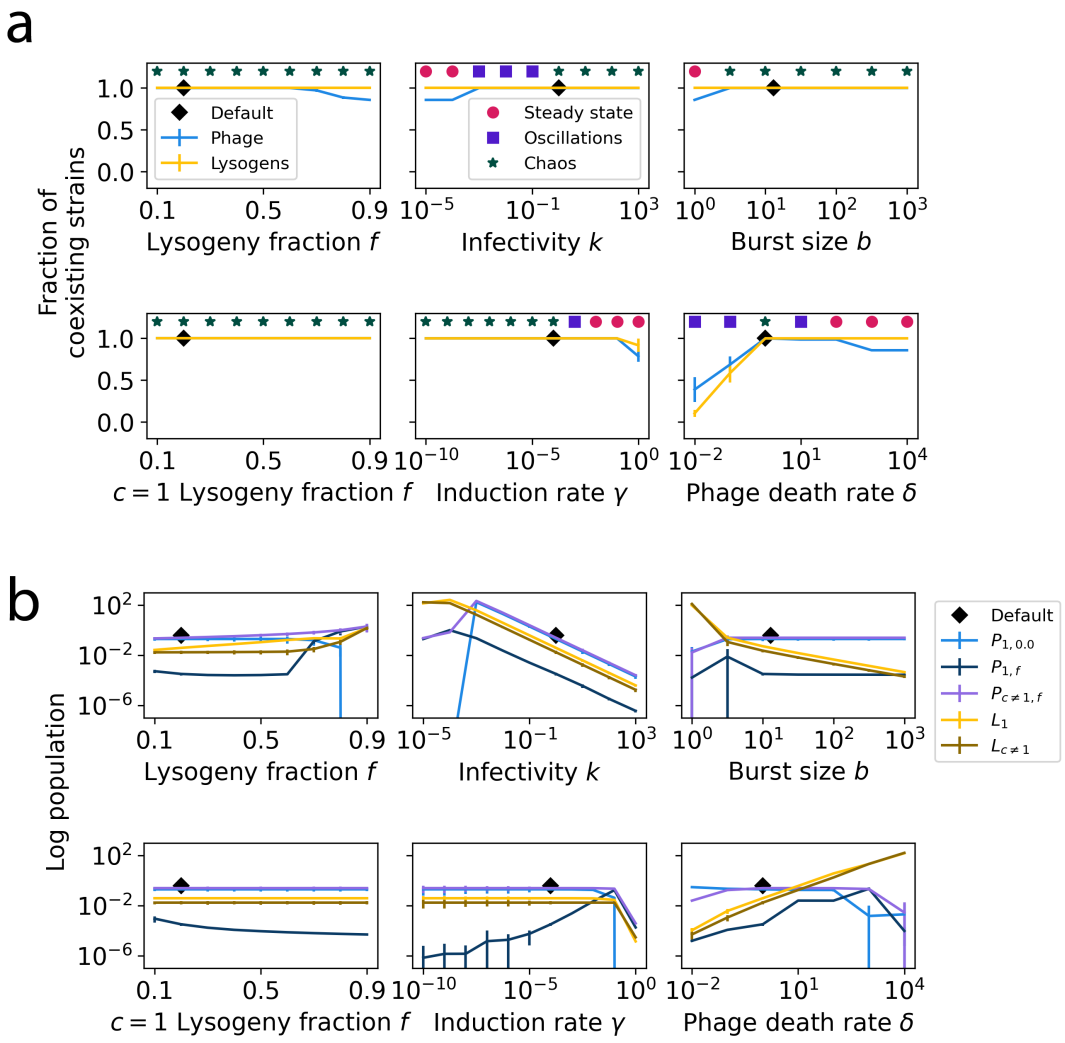

Figure S10: **One-dimensional parameter sweeps show robustness of model results to parameter changes.** We simulated the $N_c = 6$ system, with 5 immunity classes each consisting of a single temperate strain, along with a single class $c = 1$ with two strains (one obligate lytic, one temperate). Each parameter combination was simulated with 10 random initial conditions, for 10^4 timesteps (i.e. ∼14,500 generations) each. Panel **(a)** shows the fraction of strains coexisting at the end of each simulation, and the nature of the coexistence for each parameter tested (steady state: red circles; oscillatory: purple squares; chaotic: green stars); panel **(b)** shows the average population densities. Error bars show the standard error of the mean. The default parameter values used in the main text are indicated by black diamonds.

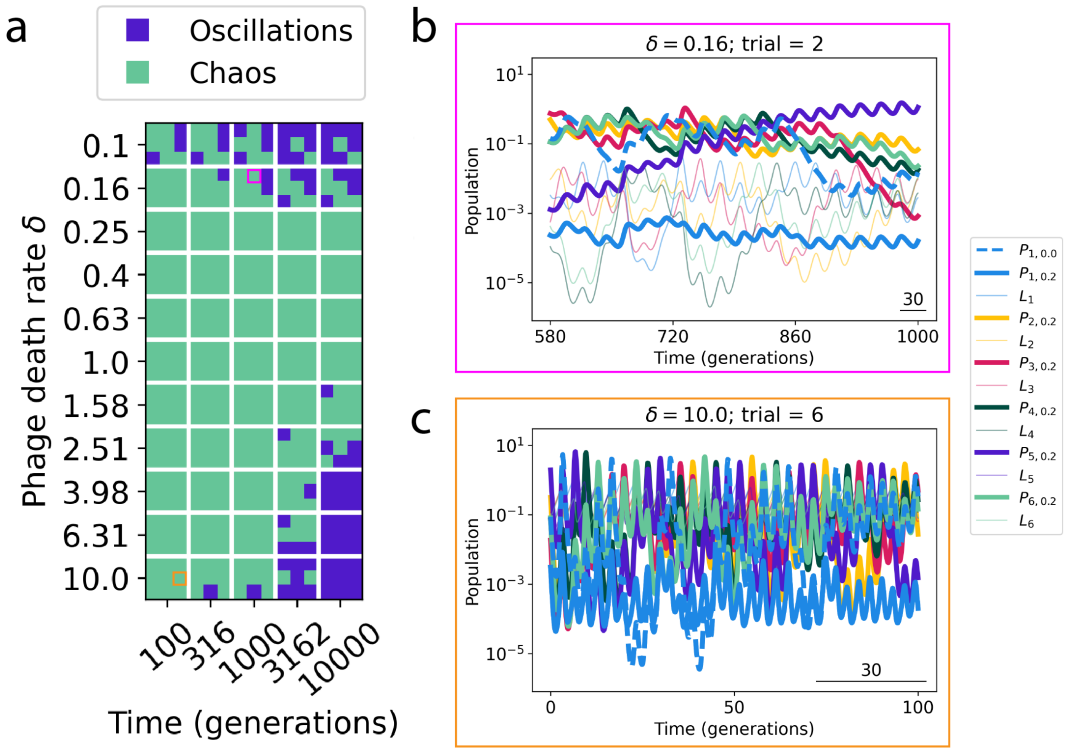

Figure S11: **Robustness of chaotic behavior observed to changes in phage death rate δ and total simulation time.** Simulations were performed for different values of δ as in Fig. S10. For each δ, simulations of 5 different lengths were performed, for 9 different initial conditions. (For each of $\delta = 0.1$ and 0.16, one initial condition led to a global extinction event; these two simulations were therefore rerun with different initial conditions.) Panel **a** shows all results for the dynamics pertaining at the end of the simulations, with each set of 9 replicates represented by a 3x3 grid. Light green squares represent chaotic trajectories; purple squares represent oscillatory trajectories. Panels **b-c** show two example trajectories, corresponding to the magenta and orange squares in panel a.

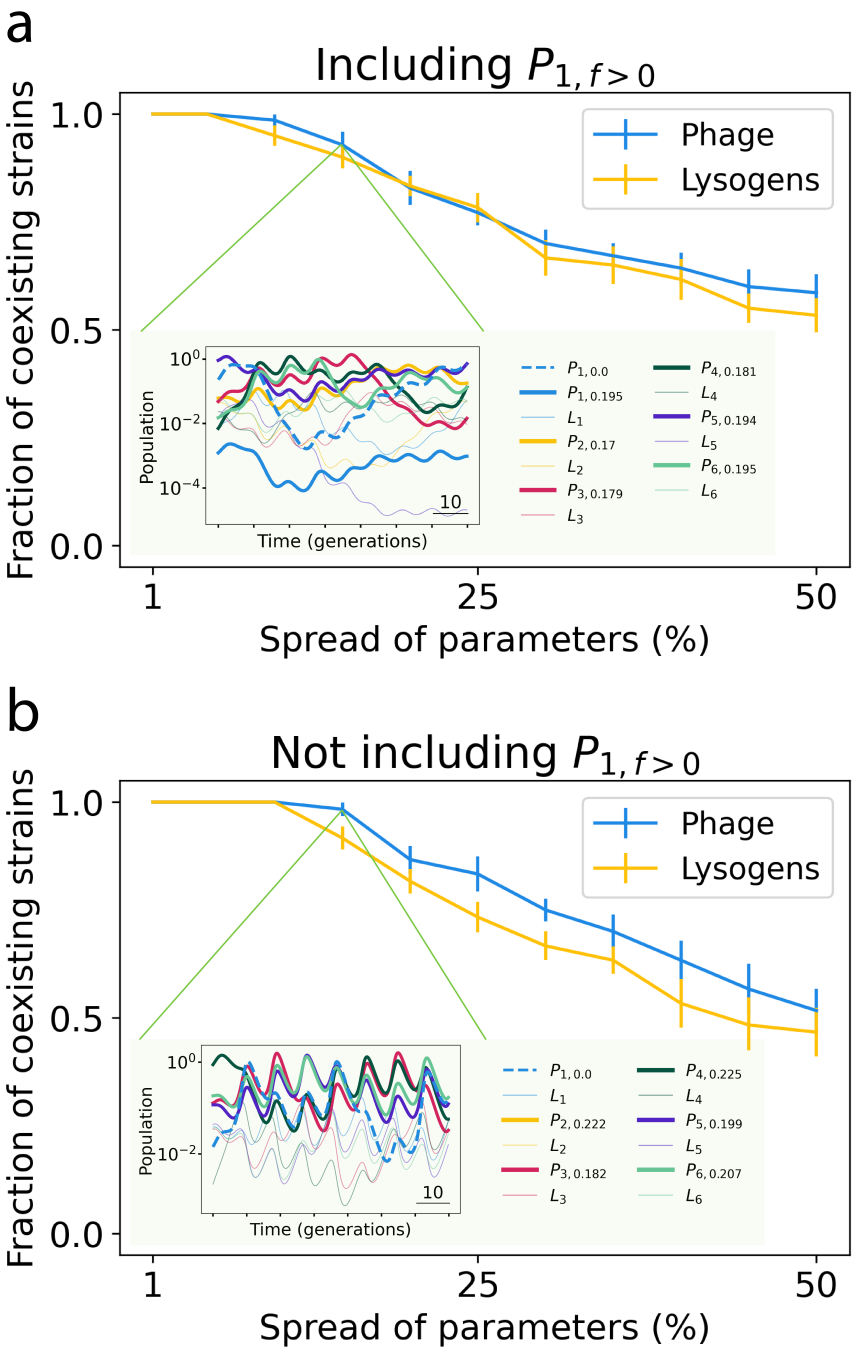

Figure S12: **Coexistence with random heterogeneous parameters.** We simulated the $N_c = 6$ system, with 5 classes each consisting of a single temperate strain, along with a single class $c = 1$ with an obligate lytic strain. **Panel a** shows results wherein class $c = 1$ includes both an obligate lytic and a temperate strain; **panel b** shows results wherein class $c = 1$ includes only an obligate lytic strain, with non-lysogenic bacteria L_1 having induction rate $\gamma = 0$ and being immune to infection by phage $P_{1,0}$. Parameters f, k, b, γ, and α were all varied randomly and uniformly from the values listed in Table S1 by between 1% and 50%. Parameters were varied heterogeneously and separately for each phage, lysogen, and phage-lysogen interaction. The fraction of strains coexisting after 10^4 timesteps (i.e. $\sim$14,500 generations) is shown. Example simulations with random parameter variations of 15% are shown. Error bars represent standard deviations across 10 trials.

S2 More comprehensive model

The model considered in the main text is a natural simplification of a more comprehensive model including both sensitive (i.e. non-lysogenic) bacteria and double lysogens. In this section, we discuss this more comprehensive approach. Main qualitative results are unchanged between the models (Fig. S6).

This model is summarized in Fig. S1, which pictorally depicts the following set of equations:

$$
\begin{aligned}
\kappa =& 1 - \Big(S + \sum_c L_c + \frac{1}{2}\sum_{c,c'} D_{c,c'}\Big)/K, \\
\frac{dS}{dt} =& \left(\alpha_S \kappa - \delta_b\right) S - kS \sum_c P_c + r \sum_c L_c, \\
\frac{dL_{cf}}{dt} =& \left(\alpha\kappa - \delta_b\right) L_{cf} + kfSP_{cf} - (\gamma + r) L_{cf} - kL_{cf} \sum_{c' \neq c} P_{c'} + r \sum_{c'} D_{cf,c'}, \\
\frac{dD_{cf,c'f'}}{dt} =& \left(\alpha_D \kappa - \delta_b\right) D_{cf,c'f'} + kfL_{c'f'}P_{cf} + kf'L_{cf}P_{c'f'} \\
& - D_{cf,c'f'}\Big[2(\gamma + r) + k \sum_{c'' \neq c,c'} \sum_{f''} (1 - f'')P_{c''f''}\Big], \\
\frac{dP_{cf}}{dt} =& b\gamma\Big(L_{cf} + \sum_{c'} D_{cf,c'}\Big) + \\
& P_{cf}\left(- k\Big[S + \sum_{c'}(L_{c'} + \frac{1}{2}\sum_{c''} D_{c',c''})\Big] - \delta + kb\left(1 - f\right)\Big[S + \sum_{c' \neq c}(L_{c'} + \frac{1}{2}\sum_{c'' \neq c} D_{c',c''})\Big]\right),
\end{aligned}
\tag{S3}
$$

where we have defined a reversion rate r for a lysogen to lose a prophage (e.g. via mutation), a carrying capacity K for bacteria (which implies an associated population-dependent growth-rate modification factor κ), a bacterial death rate δ_b, and different growth rates α_S, α, and α_D for the sensitive bacteria S, single lysogens L, and double lysogens D, respectively. The double lysogens are defined such that $D_{cf,c'f'}$ is the population density of double lysogens created by the infection of a sensitive bacterium by both P_{cf} and $P_{c'f'}$. Infection can occur in any order, such that $D_{c,c'} = D_{c',c}$ (and $D_{c,c} = 0$). As previously, we have omitted the subscript f to denote summing over the different strains of a given immunity class.

For clarity, we will now describe the origin of each term in the equation for dD/dt. The first term represents the growth and spontaneous death of double lysogens. Bacterial growth is logistic: the growth rate is reduced as bacteria become more populous and is zero at the carrying capacity K. The second and third terms represent the creation of double lysogens *via* the lysogeny of either of the two single lysogens. The fourth term represents the removal of double lysogens from the population through various means, and is itself split into separate terms: removal due to induction or reversion of either of the two lysogens; and removal due to infection and subsequent lysis by phage of a separate immunity class.

We assume that lysogens incur a small growth rate penalty, setting $\alpha_S = 1.05$ and $\alpha_D = 0.95$ (with $\alpha = 1$) [1]. We set the reversion rate r equal to the induction rate γ. Since reasonable values of the bacterial death rate δ_b are small enough that this term is negligible compared to bacterial death due to phage predation, we set $\delta_b = 0$. The results of simulations of these full equations for different values of N_c, with $K = 100$ (simulating non-limiting nutrient conditions), are shown in Fig. S6 (right panel). In these simulations, we set one immunity class to have both obligate lytic and temperate strains, and the other $N_c - 1$ immunity classes to only have a single temperate strain.

We note that this more comprehensive model lacks the perfect memory of initial lysogen populations implicit in the simplified model (equations (1)). This model yields the same qualitative results as our simplified main-text model (Fig. S7).

To recover the main-text equations from equations (S3), we make three approximations. The first of these is assuming that phage attempts to lysogenize a single lysogen result in the death of the phage rather than in the creation of a double lysogen (just as equations (S3) make an analogous approximation that neglects triple lysogens). The outcome of this approximation is that $D = 0$ for all strains, leading to the following set of equations (depicted in Fig. S13):

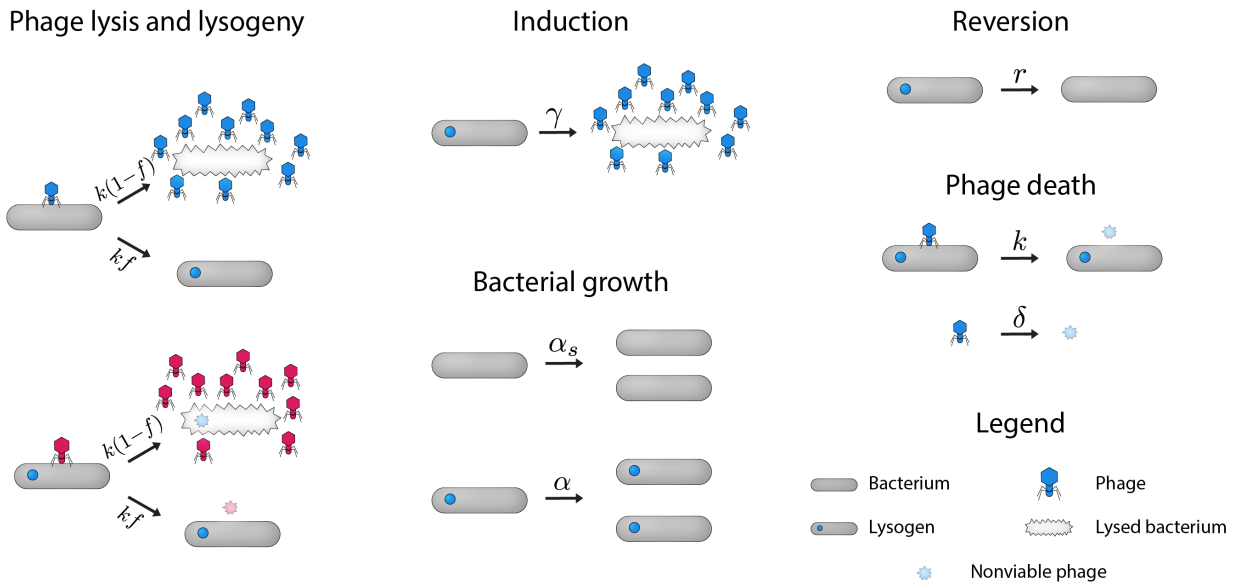

Figure S13: **Overview of model including sensitive bacteria.** A pictoral representation of the model described by equations (S4). Phage of different immunity classes are represented by different colors.

$$
\begin{aligned}
\kappa =& 1 - \Big(S + \sum_c L_c\Big)/K, \\
\frac{dS}{dt} =& \alpha_S \kappa S - kS \sum_c P_c + r \sum_c L_c, \\
\frac{dL_{cf}}{dt} =& \alpha\kappa L_{cf} + kfSP_{cf} - (\gamma + r)L_{cf} - kL_{cf} \sum_{c' \neq c} P_{c'}, \\
\frac{dP_{cf}}{dt} =& b\gamma L_{cf} + P_{cf}\left(- k\Big[S + \sum_{c'} L_{c'}\Big] - \delta + kb\,(1-f)\Big[S + \sum_{c' \neq c} L_{c'}\Big]\right).
\end{aligned}
\tag{S4}
$$

Results of simulations of these equations can be seen in Fig. S6 (middle panel). This simplification yields the same qualitative picture as the full model, with one major exception: in the full model (including double lysogens), $N_c = 2$ behaves like $N_c = 1$ in the single-lysogen model. In both cases, a single bacterial strain immune to all phage takes over the bacterial population, and leads to the extinction of obligate lytic phage strains, while temperate strains survive as a result of induction. Furthermore, $N_c = 3$ in the double-lysogen model behaves qualitatively like $N_c = 2$ in the single-lysogen model: both sometimes show oscillatory or quasi-oscillatory behavior. Finally, $N_c = 4$ in the double-lysogen model is qualitatively akin to $N_c = 3$ in the single-lysogen model: both display chaotic behavior. Thus, the model system displays chaotic behavior when there are at least two more immunity classes than the maximum allowed number of cohabiting prophage within lysogens. More generally, we find that the full model with N_c immunity classes behaves similarly to the model disallowing double lysogens with $N_c - 1$ classes.

The other two approximations made to the full model to recover the main-text equations are to: 1) assume infinite K (such that $\kappa = 1$), and 2) to set $S = 0$ (assuming zero reversion). Both are motivated by the results shown in Fig. S6, which demonstrate that: 1) predation by phage limits bacterial populations, and 2) the population of sensitive bacteria is negligible, especially for $N_c > 2$. As shown in Fig. S6 (left panel), these simplifications do not affect the qualitative behavior of the system.

S3 Finite lysis time model

In the main text, we considered a model wherein lysis is immediate. However, in nature, lysis typically occurs a time τ following infection, where $\tau \approx 2.5$ bacterial generations [2]. We therefore sought to consider a model implementing this time delay, and including a burst size of $b = 170$ (see Fig. S9). Following Ref. [3], we implemented a time delay by 10 intermediate infected states; this intermediate state model leads phage to produce a burst typically a time τ after infection (Fig. S14a). Defining $I_{cf,c'f',l}$ as the l^{th} intermediate state resulting from lytic infection of lysogen L_{cf} by phage $P_{c'f'}$, the resulting equations for this time delay model are:

$$\begin{aligned}
\kappa =& 1 - \Big(\sum_{c,f} L_{cf} + \sum_{c,f,c',f',l} I_{cf,c'f',l}\Big)/K, \\
\frac{dP_{cf}}{dt} =& \frac{10}{\tau} b \sum_{c'f'} I_{c'f',cf,10} - P_{cf}\left[\delta + k\sum_{c'f'}\left(L_{c'f'} + \sum_{c''f''l} I_{c'f',c''f'',l}\right)\right], \\
\frac{dL_{cf}}{dt} =& L_{cf}\left(\alpha\kappa - \gamma - k\sum_{c'\neq c,f'}(1-f')P_{c'f'}\right) + k\sum_{c',f'} I_{cf,c'f',1}\Theta(f'>0)\sum_{f''} P_{c'f''}, \\
\frac{dI_{cf,c'f',1}}{dt} =& k(1-f')P_{c'f'}L_{cf}(1-\delta_{c,c'}) + \gamma L_{cf}\delta_{c,c'}\delta_{f,f'} - I_{cf,c'f',1}\left(\frac{10}{\tau} + k\Theta(f'>0)\sum_{f''} P_{c'f''}\right), \\
\frac{dI_{cf,c'f',l>1}}{dt} =& \frac{10}{\tau}\left(I_{cf,c'f',l-1} - I_{cf,c'f',l}\right),
\end{aligned} \tag{S5}$$

where we have defined a carrying capacity K for bacteria (which implies an associated population-dependent growth rate modifier κ), the Kronecker delta function $\delta_{c,c'}$ which is unity if $c = c'$ and zero otherwise, and further define the Heaviside theta function $\Theta(x > 0)$ to be unity if $x > 0$ and zero otherwise. The last terms in dL_{cf}/dt and $dI_{cf,c'f',1}/dt$ express a multiplicity-of-infection feature of this model. Since phage co-infection has been shown to favor lysogeny over lysis [4, 5], in our model, when a phage infects the first intermediate state of a lytic infection caused by a temperate phage of that same immunity class, that phage infection changes from the lytic pathway to the lysogenic. As in the main text model, attempts to form a double lysogen lead to death of the infecting phage; therefore, multiplicity of infection leads the infected bacterium to revert to its pre-infection lysogenic state. A phage infecting any later intermediate state of a lytic infection has no effect on the bacterium, but results in loss of the phage.

A finite carrying capacity K is an essential feature of this time-delay model. Without a finite carrying capacity, we find that the continued growth of phage for several generations after bacteria populations start decaying typically leads to bacterial population collapse. A finite carrying capacity ensures that the amplitudes of the chaotic dynamics do not grow too large.

A recapitulation of Fig. 2 using these time-delay equations, with $b = 170$ (see Section S1) and $K = 0.2$, is shown in Fig. S8. We find that unlike in the main-text model, total lysogen population changes significantly as a function of N_c. In order to maintain that each phage has an equal probability per unit time of infecting a cell at all N_c's, we scale infectivity k with the number of phage immunity classes N_c as $k = 1/N_c$; no such rescaling was necessary for our main-text model (Fig. S14c-d).

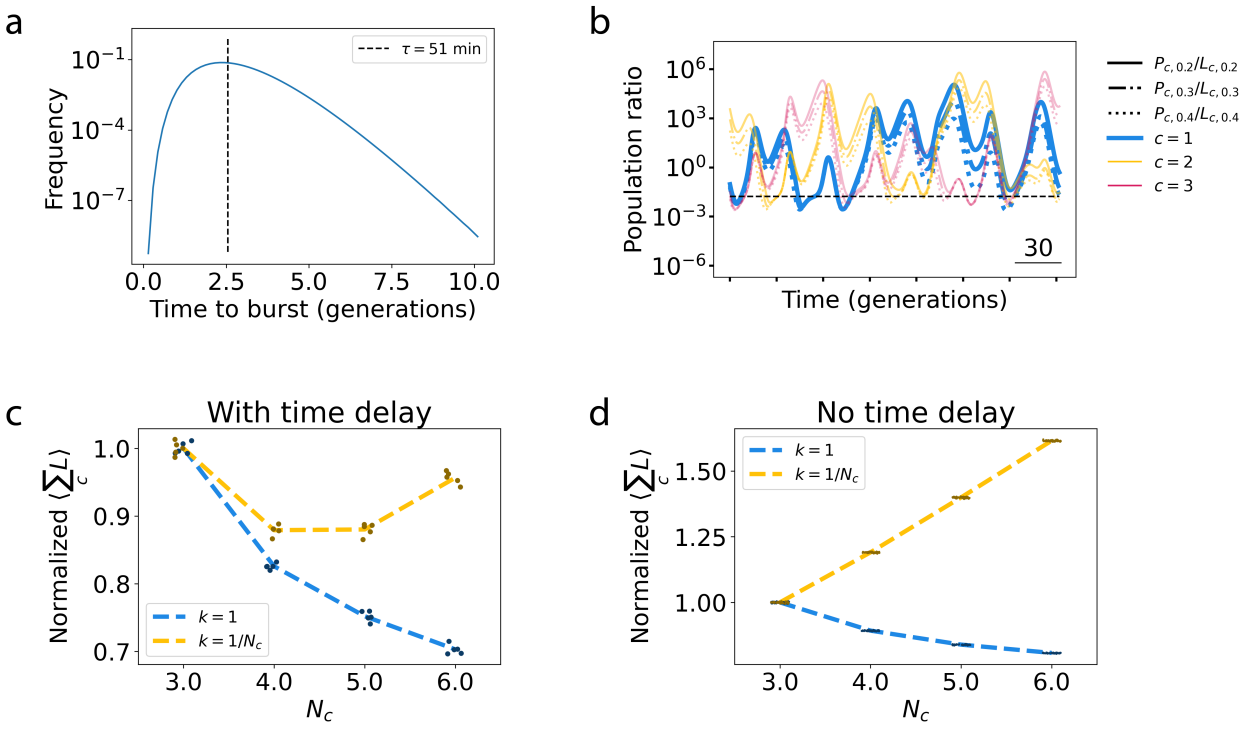

Figure S14: **Details of finite lysis time model. a,** Histogram of the time after infection leading to a burst of $b = 170$ phage. Vertical dashed line is at $\tau \approx 2.5$ bacterial generations. **b,** Ratio of population densities of phage and their corresponding lysogens, as in Fig. S8c, but where phage and lysogen population densities are compared at the same time, $P(t)/L(t)$ (rather than $P(t)/L(t-\tau)$ which is shown in Fig. S8c). **c,d** The average total lysogen population density is displayed as a function of N_c when infectivity k is either constant or scaled as $1/N_c$. For ease of comparison, lysogen population density is normalized by its average value at $N_c = 3$. Panel c shows results for the finite lysis time model (equations (S5)); panel d shows results for the main-text model (equations (1)).

S4 Chaotic behavior

Chaotic population trajectories are the predominant behavior found in the simplified model for $N_c \geq 2$, though not the only possibility: both a static fixed point and periodic oscillations sometimes occur. However, the latter have very small basins of attraction. We did not observe convergence to a fixed point in any of our simulations, but the fixed point can be solved for analytically. While simulations starting at the fixed point remain there, those that start even 1-5$\%$ away from it display chaotic behavior.

Some trajectories with $N_c = 2$ enter an oscillatory regime (as discussed above). We have also found some trajectories with $N_c = 3$, with a single temperate strain of $f = 0.2$ in each immunity class, that converge to an oscillatory regime after $10^4 - 10^5$ generations. In this case, a sudden variation of 50% in the population densities returns the system to the chaotic regime. We have never observed periodic oscillations upon introducing an obligate lytic strain to these $N_c = 3$ simulations (Fig. S15a) nor do any of the trajectories in Fig. 2f show evidence of periodic oscillations. Similarly, we never observed periodic oscillations upon introducing a fourth identical phage immunity class (Fig. S15b), nor with $N_c = 3$ immunity classes where each strain has a different lysogeny fraction (Fig. S15c).

In Fig. S16, we show various return maps, plotting how each extremum in the total phage or total lysogen population density of an $N_c = 2$ system compares to the next extremum of that population density (using the Lorenz system as a guide). The results display a fractal dimension of ~ 1.3 as calculated using a box-counting algorithm [6], consistent with chaotic dynamics.

Given that natural variations in environmental conditions would frequently induce variability into the system, and given the natural heterogeneity among different phage populations, we do not expect periodic oscillations to be biologically relevant for $N_c > 2$.

S5 Brief derivation of Eq. (3)

Here, we derive P_{cf}^{ss}, the steady-state value of P_{cf} subject to the dynamics of Eq. (1). Specifically, we assume the lysogen dynamics have reached steady state at a non-zero lysogen population L_{cf}. In this case, we have

$$\alpha - \gamma = k \sum_{c' \neq c} \sum_{f'} (1 - f')\, P_{c'f'}^{\text{ss}}. \tag{S6}$$

We consider the symmetric case in which all lysogeny fractions f' are equal and given by $f' = f$. Assuming parameter symmetries, the steady-state values of the phage population densities will be equal for different immunity classes, such that $\sum_{c' \neq c} \sum_{f'} (1 - f')\, P_{c'f'}^{\text{ss}} = (1 - f)\,(N_c - 1)\, P_{cf}^{\text{ss}}$, where N_c is the number of phage immunity classes. We thus arrive at Eq. (3),

$$P_{cf}^{\text{ss}} = \frac{\alpha - \gamma}{k(N_c - 1)(1 - f)}. \tag{S7}$$

References

[1] Michael G. Cortes, Jonathan Krog, and Gábor Balázsi. Optimality of the spontaneous prophage induction rate. Journal of Theoretical Biology, 483, 2019.

[2] Ing Nang Wang. Lysis timing and bacteriophage fitness. Genetics, 172(1):17–26, 2006.

[3] Rasmus Skytte Eriksen, Namiko Mitarai, and Kim Sneppen. Sustainability of spatially distributed bacteria-phage systems. Scientific reports, 10(1):3154, 2020.

[4] Myron Levine. Mutations in the temperate phage P22 and lysogeny in Salmonella. Virology, 3(1):22–41, 1957.

[5] Tianyou Yao, Seth Coleman, Thu Vu Phuc Nguyen, Ido Golding, and Oleg A. Igoshin. Bacteriophage self-counting in the presence of viral replication. Proceedings of the National Academy of Sciences of the United States of America, 118(51), 2021.

[6] Francesco Turci. Box Counting in Numpy. https://francescoturci.net/2016/03/31/box-counting-in-numpy/, 2016.

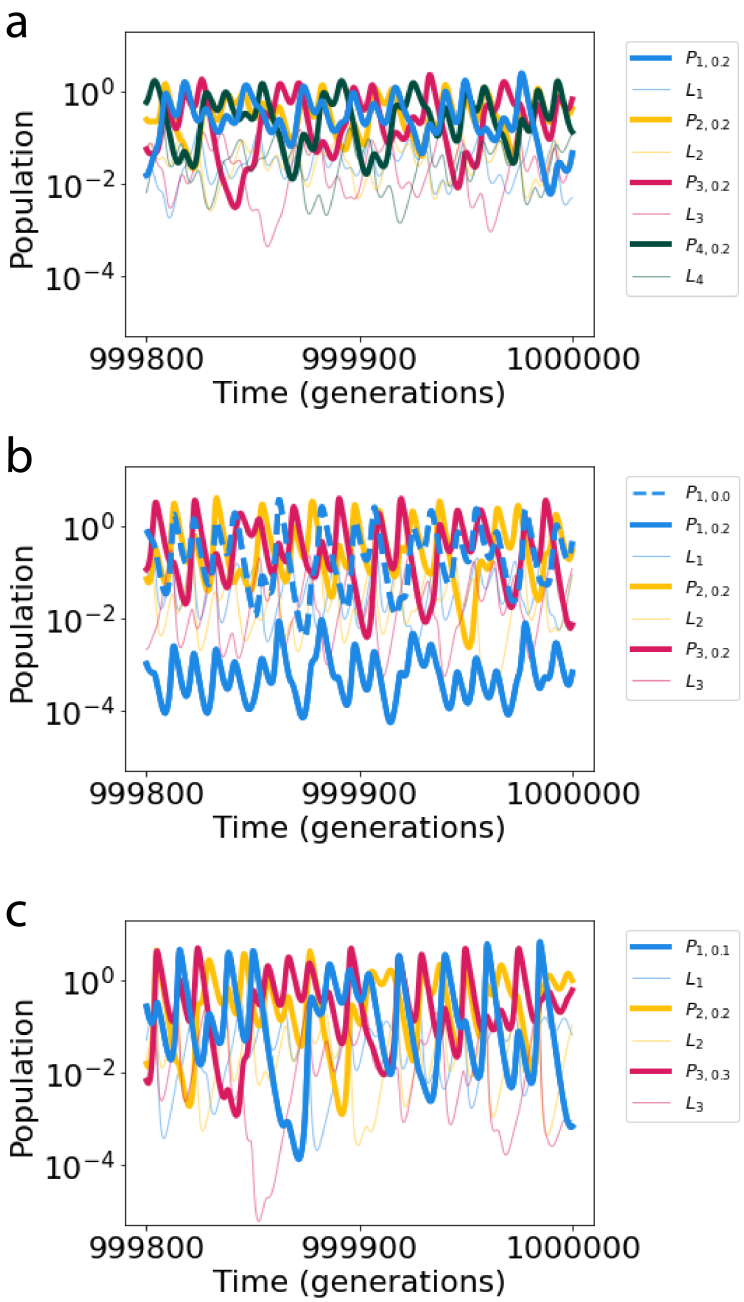

Figure S15: **Chaotic trajectories are typical.** **a,** Simulation with $N_c = 4$ phage immunity classes, each with a single temperate strain with lysogeny fraction $f = 0.2$. **b,** Simulation with $N_c = 3$ phage immunity classes, one of which has two strains—one obligate lytic and one temperate ($f = 0.2$)— and two of which have a single temperate strain ($f = 0.2$). **c,** Simulation with $N_c = 3$ phage immunity classes, each with a single temperate strain of different lysogeny fractions.

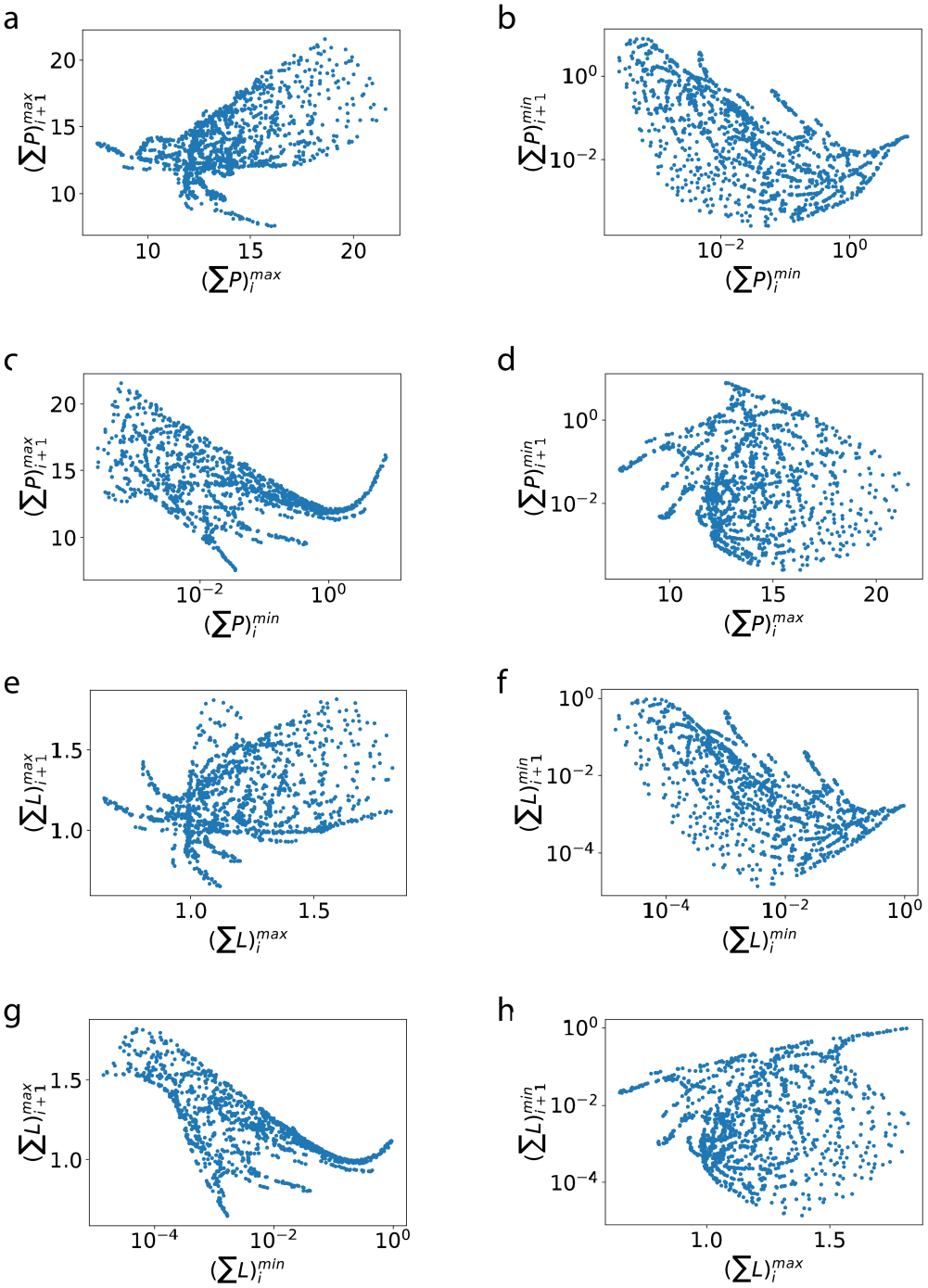

Figure S16: **Return maps for an $N_c = 2$ system, using equations** (1). **a,** Comparison of each maximum of total phage population density to the next maximum. **b,** Comparison of each minimum of total phage population density to the next minimum. **c,** Comparison of each minimum of total phage population density to the next maximum. **d,** Comparison of each maximum of total phage population density to the next minimum. **e,** Comparison of each maximum of total lysogen population density to the next maximum. **f,** Comparison of each minimum of total lysogen population density to the next minimum. **g,** Comparison of each minimum of total lysogen population density to the next maximum. **h,** Comparison of each maximum of total lysogen population density to the next minimum.